

# Effects of Highly Non-uniform Illumination Distribution on Electrical Performance of Solar Cells

E.T.Franklin, J.S Coventry  
Centre for Sustainable Energy Systems  
Australian National University  
Canberra ACT 0200  
AUSTRALIA

Telephone: +61 02 6125 3976  
Facsimile: +61 02 6125 0506  
E-mail: [evan@faceng.anu.edu.au](mailto:evan@faceng.anu.edu.au)

## **Abstract**

Conventional thinking for cells under concentrated sunlight would suggest that short circuit current, and hence also open circuit voltage, can be determined exactly by the total illumination falling onto the cell. However with most concentrator systems the cells are exposed to highly focused light, with consequent non-uniform temperature and current distributions. Departures from the simple relationship are then observed. Starting from the current density – voltage relationship for any given cell position, a detailed examination is made of junction voltage and current as functions of position, and an overall cell I-V curve is produced for a given illumination distribution.

## **1 INTRODUCTION**

The simplest approach to design and prediction of performance for a cell under concentrated illumination is to assume that the flux distribution is uniform across the whole area of the cell and is equal to the average concentration ratio multiplied by the illumination magnitude at one sun intensity. For real concentrator systems, however, the illumination intensity rarely exhibits such uniformity across the cell. In this paper the case of gaussian illumination flux distribution is considered, an illumination profile which can be modelled and observed for a concentrator system consisting of reflective troughs.

Cells under concentrated sunlight have large currents, therefore particular attention must be paid to series resistance which is distributed in nature. The main sources of resistance within a conventional front-illuminated solar cell are the metal grid, the finger/emitter contacts, the shallow emitter region, the bulk region, the rear contacts and the rear metal. Since it is possible to build a relatively thick rear metal layer with large area coverage, the rear metal resistance can be made negligible. The rear semiconductor/contact resistance can also be kept small through the use of localised rear surface doping.

The effects of distributed series resistance for uniform illumination can be considered by defining an equivalent lumped series resistance and then modelling the cell with the solar cell equivalent circuit (Nielsen 1982; Sokolic et al. 1993). However, the equivalent lumped resistance value actually depends upon the illumination level. It in fact varies significantly with photocurrent density and with operating point (Araujo et al. 1986). For this reason alone, the simple lumped method does not adequately model distributed illumination. The lumped equivalent circuit also does not take into consideration the so-called ‘distributed diode effect’. Distributed resistance results in the junction voltage varying with position, and hence generated current varying with position also.

As will be shown in this paper, the non-uniform light distribution not only affects the fill-factor but also results in an open circuit voltage reduction. This effect has been previously observed through experiment by Cuevas et al. (1983), for the case of uniform illumination with partial cell shading. The reduction in open-circuit voltage becomes larger for more centralised illumination distributions.

A further dimension is considered in this paper with the inclusion of a temperature distribution within the cell, the

inevitable result of exposure to real concentrator conditions. The effect of temperature on solar cell performance, open circuit voltage and short circuit current, has been dealt with by many texts (Goetzberger et al. 1994 or Wenham et al. 1994 for example). This paper extends the study of temperature by examining the effect of a temperature distribution within the cell.

The illumination profile conditions are based upon tracking trough concentrators that are used by the ANU’s Centre for Sustainable Energy Systems in their Combined Heat and Power Solar (CHAPS) systems (Coventry et al. 2002). The cells are cooled by a water channel. The modelled cell temperature distribution is obtained by a 2-D heat transfer model of the CHAPS receiver. The modelled cell is based upon the high efficiency mono-crystalline concentrator cells manufactured and used by the ANU’s Centre for Sustainable Energy Systems, and designed for use with a concentration ratio of approximately 30 suns.

Also included in this paper are some experimental cell I-V curves for a cell under conditions of uniform light and a centralised distribution of light. The curves were measured in the laboratory, with the cell being held at a constant and uniform temperature, and qualitatively reveal the open-circuit voltage reduction as modelled.

## 2 MODEL

### 2.1 Illumination Profile

Tracking concentrators often do not produce a uniform flux density distribution at the output aperture. A parabolic trough concentrator, for example, produces a flux distribution that closely resembles the gaussian curve. Figure 1a shows a plot of light intensity distribution across the target width, using OptiCAD ray-tracing software to model the CHAPS system optics (Opticad Corporation 2001). During practical sun-tracking operation, this profile slowly moves across the cell (between discrete alignments of the tracking system) and so is not always perfectly centered. The current modelling, however, is restricted to the case of a centered illumination distribution profile.

The actual intensity profile produced at the target region for one of the earlier ANU CHAPS systems has been observed by photogrammetry methods by Burgess (Burgess et al. 2002), with plots of flux intensity vs. target position plots taken at different positions along the receiver length. These measurements confirm the approximate gaussian shape, an example of the distribution shown in Figure 1b. The measured profile has a lower peak than the modelled profile, and a sharper drop off on one side (which may indicate an off-track situation at the time of the photogrammetry capture). The mean concentration ratio in this case was measured to be 22.7 averaged across the 40mm cell width, which is 30% lower than is expected for the next generation of mirrors. The illumination profile used in the complete modelling of illumination intensity and temperature effects is closely based upon the measured results.

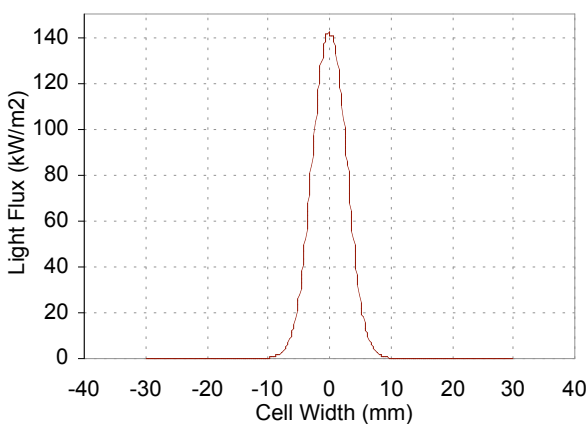


Figure 1a. Modelled light flux intensity at the focal region for a 1.2m wide mirror

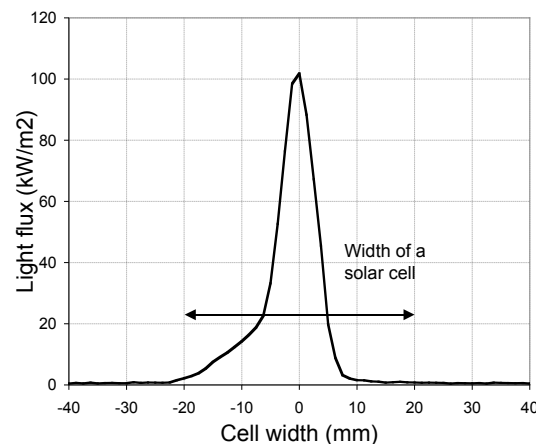


Figure 1b. Measured light flux intensity at the focal region for a 1.2m wide mirror

### 2.2 Temperature Distribution

The process of light being absorbed by a photovoltaic cell entails incoming high energy photons creating electron-hole pairs. Depending upon the wavelength, only a fraction of the photon’s energy is actually required to generate the electron-hole pair, with any excess energy being quickly dissipated to the silicon lattice as heat. Since the high energy, short-wavelength photons are absorbed in the first few microns of the cell, the majority of this generated heat is

effectively injected into the lattice at the front surface. The theoretical maximum fraction of incoming energy that can be converted into electrical energy, and hence not contribute to heat generation, is about 30% for a single junction silicon cell. However in reality, very good, high-production level mono-crystalline cells are currently capable of converting up to around 23% of the incoming energy. If the bulk of heat generation occurs in the central region of a cell it follows that this region will be operating at the highest temperature.

The actual determination of temperature profile throughout the silicon material has been carried out at ANU using Strand7 modelling software to model the CHAPS receiver configuration (Coventry et al. 2002). A gaussian illumination profile has been used, assuming that 75% of total incoming energy is injected as heat at the front surface of the cells. Results of the receiver thermal modelling for 55°C turbulent water flow with a light external breeze are shown in Figure 2. The temperature profile closely resembles the gaussian distribution, with a temperature difference of about 14°C between the centre and the outer edge of the cell.

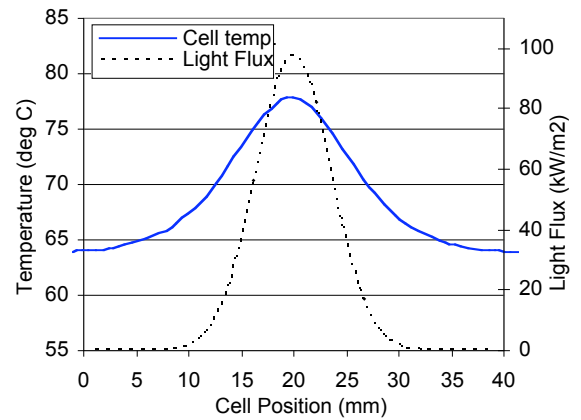


Figure 2. Modelled cell temperature vs. position

### 2.3 Cell Model - Distributed Resistance

Due to the large generated currents but small operating voltages which are typical for cells under concentration, the minimisation of series resistance is of crucial importance. The major visible difference between a cell designed for one-sun intensity and a cell designed for concentrated sunlight applications is front metal grid spacing, aimed at reducing the resistance of the emitter/grid region. The cell used in this model is based upon cells manufactured and used at ANU for the CHAPS system, and is typical of a cell designed for an average concentration ratio of 20 – 50 suns. The cell can be considered to comprise of a number of identical ‘quarter finger-space’ units, so that to model the entire cell it becomes necessary only to consider one of these units. The dimensions and key physical properties of the unit cell are shown in Figure 3. The entire cell behaviour is determined by the accumulation of each of these identical units, ignoring the surface recombination effects at the outer edges of the entire cell. The concentrator cells at ANU consist of 170 fingers, and there are thus 680 of these identical units.

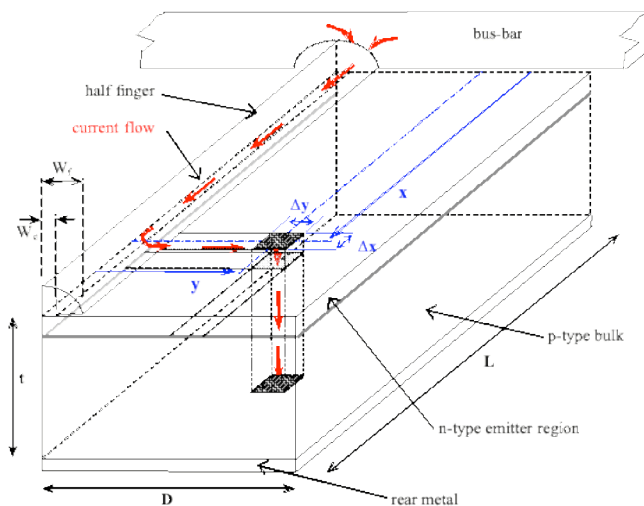


Figure 3. Quarter finger-space cell unit with element  $\Delta x$  by  $\Delta y$  at position  $(x, y)$

For a small enough element size the current density remains virtually constant across the element and so the current attributable to the element area is simply determined by the respective current density at  $(x,y)$  multiplied by the element area,  $\Delta x.\Delta y$ . Also, since the illumination and temperature only vary across the width of the cell (in the  $x$ -direction), the photocurrent density,  $J_L$ , the temperature,  $T$ , and the reverse saturation current density,  $J_0$ , become independent of  $y$  and the equation can be re-written:

The net current generated by the rectangular cell element at position  $(x, y)$ , as defined by  $\Delta x$  and  $\Delta y$ , is given by the single diode solar cell equation:

$$I_j(x, y) = I_0(x, y) \left[ e^{\frac{q.V_j(x,y)}{K.T(x,y)}} - 1 \right] - I_L(x, y) \quad (1)$$

where  $I_j(x, y)$ ,  $I_0(x, y)$ ,  $I_L(x, y)$ ,  $V_j(x, y)$ ,  $T(x, y)$  are the net current flowing across the junction, the reverse saturation current, the photocurrent, the p-n junction voltage and the temperature respectively for the given element position  $(x,y)$ . An ideality factor of 1 is assumed. For positions directly beneath the metalised fingers we simply have a ‘dark’ diode which generates current governed by the same equation but with  $I_L(x, y) = 0$ .

$$I_j(x, y) = J_0(x) \exp\left(\frac{q \cdot V_j(x, y)}{K \cdot T(x)}\right) - J_L(x) \quad , \quad y > W_f \quad (2)$$

$$I_j(x, y) = J_0(x) \exp\left(\frac{q \cdot V_j(x, y)}{K \cdot T(x)}\right) - 1 \quad , \quad y < W_f \quad (3)$$

The standard convention is observed for current flow direction, a positive current being one that flows from the p-type to the n-type silicon. In normal ‘generating’ mode of course the current is in fact negative and flows from the front to the rear of the cell (n to p). The current densities  $J_L$  and  $J_0$  are variable with position in the x-direction through their dependence on temperature  $T(x)$ . The simple expressions used are based on a linear increase in photocurrent with increasing temperature and a constant rate of open circuit voltage decline with increasing temperature, where the temperature coefficients can either be taken from theory or measured using test cells:

$$J_L(x) = J_{L_{300}}(x) (1 + C_1 \cdot (T(x) - 300)) \quad (4)$$

$$J_0(x) = \frac{J_{L_{avg}}}{\exp\left(\frac{q}{K \cdot T(x)} \left( \frac{300 \cdot K}{q} \ln\left(\frac{J_{L_{avg}}}{J_{0_{300}}(x)}\right) + C_V(T(x) - 300) \right)\right)} \quad (5)$$

where  $J_{L_{300}}(x)$  and  $J_{0_{300}}(x)$  are the position specific photocurrent density and reverse saturation current density at a temperature of 300K.  $C_1$  and  $C_V$  are the temperature coefficients for photocurrent and open-circuit voltage respectively, the values of which can either be taken from theory or measured from a cell’s characteristics under uniform illumination conditions at various temperatures.  $C_V$  is of course negative since the open circuit voltage decreases with increasing temperature.  $J_{L_{avg}}$  is a constant, the average photocurrent, used in equation (5) to calculate the local open circuit voltage and hence the temperature adjusted reverse saturation current  $J_0(x)$ , which increases with temperature but is otherwise kept independent of illumination level.

Each of these generated element currents,  $I_j(x, y)$ , must pass from the rear metalised surface through the resistive bulk to the junction, laterally through the shallow emitter region, into the finger and finally along the finger to the bus-bar, with voltage drops associated with each part of this current path. Both the rear metal surface and the bus-bar are each assumed to be equipotential, with the ‘overall’ cell voltage being the difference in potential between these two contacts.

Despite the illumination level changing with position across the cell, and hence current generation varying with position, simplifying assumptions can be made about the current flow by taking advantage of the geometry of the ‘quarter finger-space’ unit. Keeping in mind that the dimensions of the unit in Figure 3 are 20mm x 0.15mm, a long thin region of emitter, the illumination intensity (and hence generated current) can be considered to vary only gradually in the x-direction. The resistivity of the silver finger is several orders of magnitude less than the emitter region, and so with neighbouring elements generating virtually equal magnitudes of current, the current will travel directly to/from the finger. The emitter resistance results in a junction voltage that increases with distance from the finger. As a consequence regions closer to the finger contribute a higher net current to the cell’s output. This is often referred to in literature as ‘current-crowding’, and the effect becomes more noticeable the higher the emitter sheet resistance. The current crowding effects are still not fully accounted for though by this model because there can also be a component of minority carrier diffusion laterally through the bulk, as discussed by Aberle et al. (1993), which further reduces the current contribution from regions distant from the fingers. Future 3-dimensional modelling is planned to resolve the full consequence of this process.

A similar assumption can be made about the movement of current through the bulk, from the junction to the rear metal. The thickness of the bulk region is typically between four and five hundred microns, small in comparison with the width of the cell. Since for a gaussian illumination the generated current density will not differ significantly between neighbouring elements, the current will primarily flow directly to the rear surface. If the rear surface is not completely metalised, as is the case for a lot of real cells, then the actual resistance path will be longer. In this model the assumption of full rear metal coverage with zero contact resistance, and a bulk thickness of 400 microns is made.

The solution for the unit cell becomes an iterative one with the junction voltage for each element being determined by solving the resistive network represented in Figure 4, where the generated current contribution  $I_j(x, y)$  for each element is itself dependant upon the solution of the resistive network and the position dependent solar cell equations (2) and (3).

The network is reduced to a matrix expression and solved using a controlled iteration procedure with the overall cell voltage held at a constant value. The solution is repeatedly determined over a range of cell voltages to build up an I-V curve. This process has been implemented in visual basic code, using MS Excel as an input/output interface, with the full set of parameters listed in Table 1.

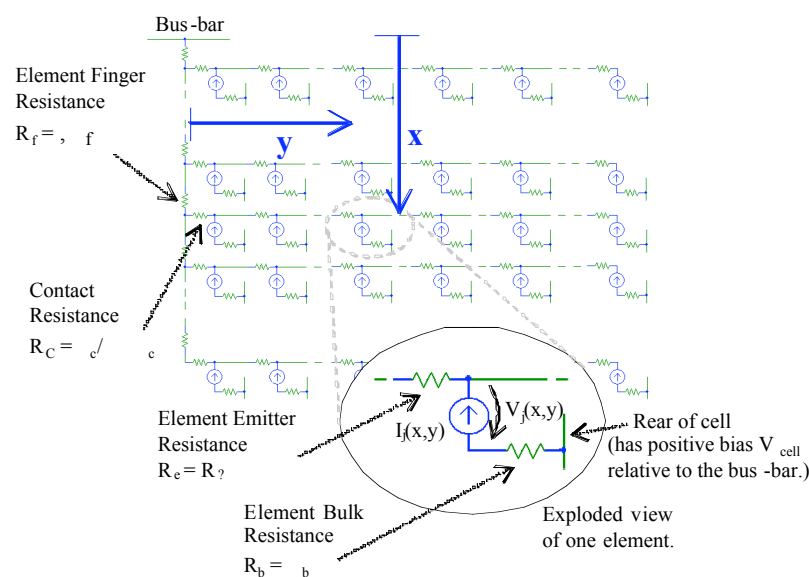


Figure 4. Representation of the resistive network – an array of  $(L/\Delta x)$  by  $(D/\Delta y)$  elements

<b>Resistivities:</b>	
Bulk, $R_b$	0.5 ohm.cm
Emitter sheet, $R_e$	120 ohms/square
Finger, $R_f$	0.44 ohms/cm
Contact, $R_c$	$10^{-4}$ ohm.cm <sup>2</sup>
<b>Dimensions:</b>	
Half-finger length, $L$	19mm
Half-space width, $D$	150 $\mu$ m
Half finger width, $W_f$	12 $\mu$ m
Contact width, $W_c$	4 $\mu$ m
Bulk thickness, $t$	400 $\mu$ m
<b>PV characteristics:</b>	
$J_0$ @ 1 sun, 300K	$6 \times 10^{-13}$ A/cm <sup>2</sup>
$J_L$ @ 1-sun, 300K	36 mA/cm <sup>2</sup>
$V_{OC}$ temp coeff, $C_V$	-2 mV/°C
$I_{SC}$ temp coeff, $C_I$	0.0008 /°C

Table 1. Unit cell parameters

## 3 RESULTS

### 3.1 Modelled Results

Using a large number of divisions per unit cell (5000 in the x-direction and 100 in the y-direction, giving an element size of 3.8  $\mu$ m x 1.5  $\mu$ m) and with decreasing overall cell voltage step-sizes, I-V curves are produced. Using the parameters in Table 1, the cell has an open-circuit voltage of 724mV and an efficiency of 19.9% for uniform light (concentration = 22.7) and a uniform temperature of 25°C. The three I-V curves of Figure 5 correspond to three cases: uniform illumination and uniform temperature distribution, distributed illumination and uniform temperature, and distributed illumination and distributed temperature. In each case the same amount of light is absorbed by the cell (at an average concentration ratio of 22.7), and the average cell temperature is also identical (69°C). The illumination and temperature distributions are gaussian in nature corresponding to those discussed in section 2.1 and 2.2. The section of curves plotted commence at 400mV, as the curves below this point are almost flat. In actual fact there is a marginal increase in short-circuit current for the distributed temperature case due to the slight increase in generated photocurrent with temperature and owing to the fact that there is a higher illumination in the hotter region of the cell. When the distributed illumination is introduced (with the net illumination remaining identical) there is a reduction in open circuit voltage. When the cell is modelled to include both distributed illumination and temperature, there is a further reduction. The knee of the I-V curve can also be seen to 'soften' slightly, indicating the increased effect of series resistance. The difference between open-circuit voltage for the case of uniform illumination and temperature and for the case of distributed illumination and uniform temperature is around 5mV, with a further reduction of 2mV when distributed temperature is included. The cell efficiency reduces from 17.3% for uniform illumination and temperature, to 16.8% for distributed illumination and uniform temperature, and 16.7% for distributed illumination and temperature.

Figure 6 shows the variation in open circuit voltage and efficiency with illumination profile. The output characteristics have been modelled using small increments in overall cell voltage and the open-circuit voltage and maximum power point determined for a range of illumination conditions. In each case, the total amount of light absorbed by the cell remained identical (with an average concentration ratio of 30), the temperature is kept uniform throughout the cell at 30°C for each simulation. The illumination distribution is defined by a centered gaussian profile in each case, with the peak intensity being varied between 30x concentration (i.e. a uniform illumination profile) and 240x concentration (a highly central profile). The peak concentration of the distributed illumination divided by the average concentration (30 suns) is referred to in the plots as 'Peak Illumination Ratio'. Open-circuit voltage and efficiency both decrease significantly with increasing peak illumination, i.e. with increasingly centralised illumination profile.

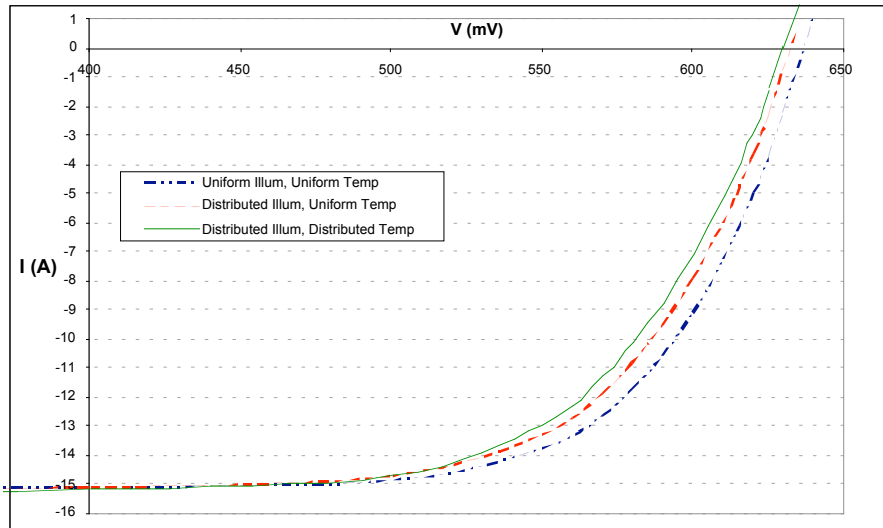


Figure 5. Simulated I-V Curves: average concentration ratio = 22.7, average temperature = 69°C

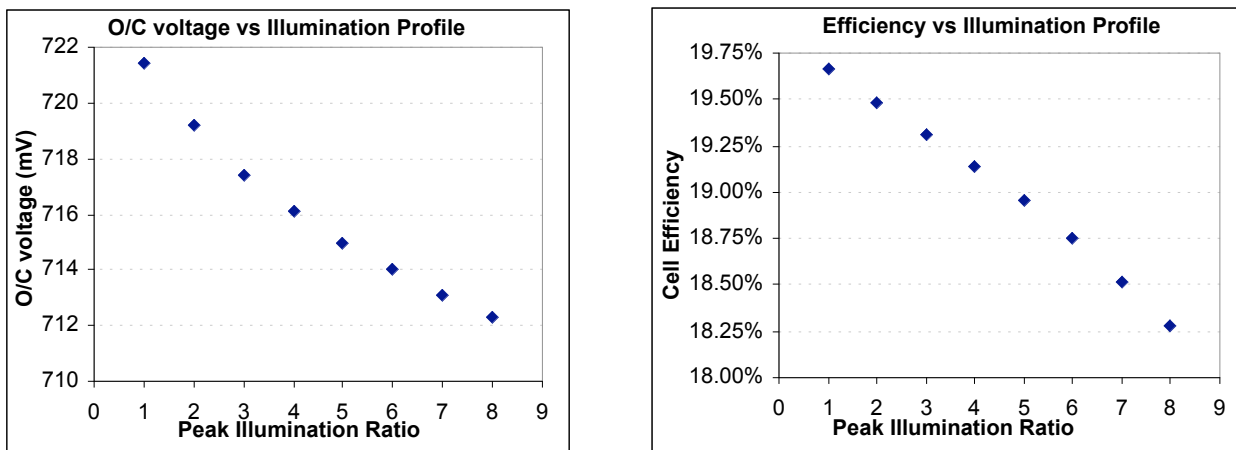


Figure 6. Open-circuit (O/C) Voltage and Efficiency variation with peak illumination intensity, for gaussian illumination distribution with an average concentration ratio of 30, and a uniform cell temperature of 30°C.

It is interesting to look at what is actually happening in the cell at open-circuit. By definition open-circuit refers to the condition where no net current flows into or out of the cell, but there are in fact currents flowing within the cell. A convenient current to observe is the current entering the fingers at each position along the fingers, and also the net current flow within the fingers as a function of position. Rather than look at the currents for one quarter finger on its own it is more meaningful to look at the sum of finger currents. These current distributions are shown in Figure 7 for the case of distributed illumination and temperature profiles, as discussed in section 2.1 and 2.2, with the cell at open-circuit. In the region furthest from the bus-bar, where the cell is most heavily illuminated, a current is leaving the finger (due to the generated photocurrent in that region of cell), whilst in the region near the bus-bar current is entering the finger. The illuminated region is generating current and has not yet reached local open-circuit, and this current is then supplied to the dark region which has been driven past local open circuit and is sinking current as a result. The net result is a significant current flow between the two regions (the solid line in Figure 7). The net current is zero at the bus-bar, since of course the entire cell is operating at open-circuit, but increases to a maximum of about 4.5 amps (significant considering the short circuit current is in the order of 15 amps) at roughly two thirds of the distance to the centre of the cell.

Along with non-zero current flows at open circuit, all points of the cell are of course not equipotential. Figure 8 shows a plot of junction voltage over the area of the quarter-finger cell unit. The scale in the y-direction (distance from finger) has been enlarged so that the potential distribution can be represented in three-dimensions as shown. Even at open-circuit the junction voltage varies quite markedly across the cell, with the central, highly illuminated region operating at a higher voltage (despite not yet reaching local open-circuit voltage).

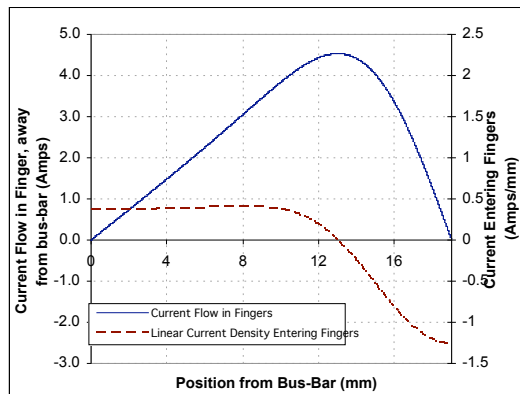


Figure 7. Current distributions at open-circuit

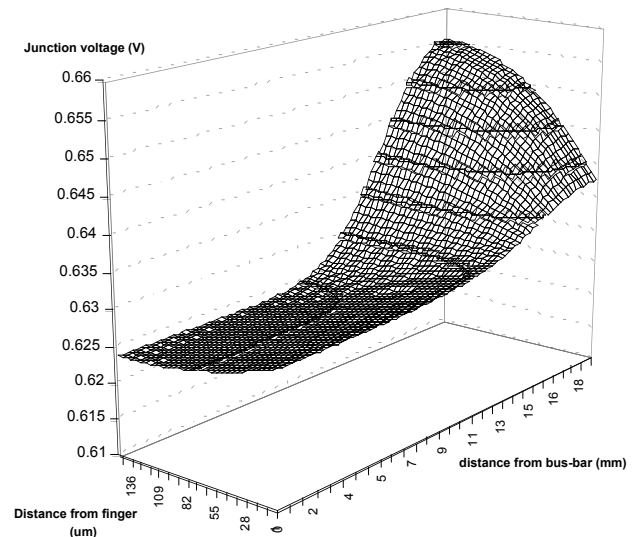


Figure 8. Junction voltage throughout unit cell at open-circuit

### 3.2 Experimental Comparison

A cell has been tested in the laboratory at ANU, under simulated concentrated sunlight conditions. The cell is encapsulated, in the same manner as for an entire CHAPS receiver, and is measured to be 20.9% efficient with a uniform illumination of 30 suns on the top glass cover. The testing has been carried out using the ANU Flash-Tester (Keogh 2002) which exposes the cell to a calibrated light intensity for short periods of time. Water channels behind the cell are used to maintain a constant temperature, and the short light exposure times ensure that the temperature throughout the cell remains uniform. The cell parameters ( $J_0$ ,  $J_L$  and Resistances) will not be identical to those of the modelled cell (which are typical values rather than being specific for this one cell). In addition, a step illumination profile is applied (achieved by masking the outer sides of the cell) rather than the gaussian profile that is used in the model, and so no exact quantitative comparison can be made. Instead, it is possible to make a qualitative comparison of the modelled and observed results. The measured I-V curves are plotted in Figure 9. The dashed curves correspond to a uniform illumination intensity of 30 suns across the entire cell area, whilst the solid curves correspond to a light intensity of 90 suns over just the central third of the cell. The short circuit current is the same in both cases since the cell receives identical amounts of light in each case, and the cell temperature is maintained at 17°C. A reduction in open circuit voltage of 7mV was observed. The cell efficiency was also observed to drop significantly, from an average of 20.9% for uniform illumination to 20.0% for centralised illumination.

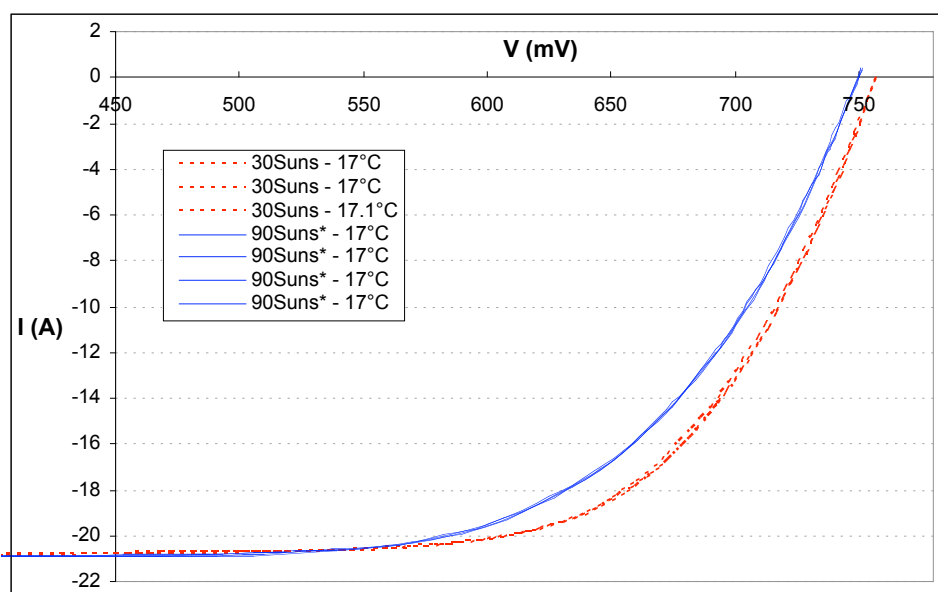


Figure 9. Measured I-V curves for uniform and central illumination

## 4 CONCLUSIONS

The modelling of this work has shown that a cell under non-uniform focused illumination, as produced by many concentrator systems, experiences a drop in both open-circuit voltage and efficiency compared to a cell under uniform illumination, despite the cell receiving identical total illumination in each case. The reduction becomes larger with increasingly centralised illumination profile. A real situation has been modelled, taking into account temperature differentials between the highly illuminated and less illuminated regions of the cell, and the results show a further reduction in open-circuit voltage and a further softening of the I-V curve. Re-injection of carriers through the pn junction and diffusive flow of minority carriers within the base has been ignored in this modelling. Further work using a 3D model will take these effects into account.

Experimental I-V curves for uniform and non-uniform illumination also revealed significant reductions in open circuit voltage and efficiency, providing good evidence to support the modelled results.

The lumped series resistance model for a solar cell does not account for this reduction in open circuit voltage and efficiency with changes in illumination intensity profile. The basic assumption that open-circuit conditions equate to zero current flow is shown to be flawed for real concentrator cells, with internal current flows becoming significant for non-uniformly illuminated cells.

## 5 ACKNOWLEDGMENTS

The work described in this paper has been supported by the Australian Cooperative Research Centre for Renewable Energy (ACRE). ACRE's activities are funded by the Commonwealth's Cooperative Research Centres Program. Evan Franklin and Joe Coventry have been supported by ACRE Postgraduate Research Scholarships.

## 6 REFERENCES

- Aberle, A. G., Wenham, S. R. and Green, M. A. (1993). *A New Method for the accurate measurement of the lumped series resistance of solar cells*. IEEE PS Conference Proceedings 1993.
- Araujo, G., Cuevas, A. and Ruiz, J. (1986). *The Effect of Distributed Series Resistance on the Dark and Illuminated Current-Voltage Characteristics of Solar Cells*. IEEE Transactions on Electron Devices. 33.-3. pp.391-401.
- Burgess, G. and Johnston, G. (2002). *Personal Communication: Photogrammetry Data for CHAPS 1 Mirror*. Canberra. (greg@faceng.anu.edu.au).
- Coventry, J. S., Franklin, E. and Blakers, A. (2002). *Thermal and electrical performance a concentrating PV/Thermal collector: results from the ANU CHAPS collector*. ANZSES Conference 2002. Newcastle, Australia.
- Cuevas, A. and Lopez-Romero, S. (1983). *The Combined Effect of Non-uniform Illumination and Series Resistance on the Open-Circuit Voltage of Solar Cells*. Solar Cells. 11. pp.163-173.
- Goetzberger, A., Knobloch, J. and Voss, B. (1994). *Crystalline Silicon Solar Cells*. John Wiley & Sons.
- Keogh, W. M. (2002). *Accurate Performance Measurement of Silicon Solar Cells*. PhD Thesis. The Australian National University.
- Nielsen, L. D. (1982). *Distributed Series Resistance Effects in Solar Cells*. IEEE Transactions on Electron Devices. 29.-5. pp.821-827.
- Optical Corporation (2001). *OptiCAD - Optical Analysis Program, v7.0*. Santa Fe.
- Sokolic, S., Krizaj, D. and Amon, S. (1993). *Lumped Series Resistance of Solar Cells as a result of Distributed Sheet Resistance*. Solid-State Electronics. 36.-4. pp.623-630.
- Wenham, S. R., Green, M. A. and Watt, M. E. (1994). *Applied Photovoltaics*. Centre for Photovoltaic Devices and Systems.